AD-A274 779

(2)

BREAKWIRE TECHNIQUE FOR HYPERVELOCITY MEASUREMENT

AR-008-223

MICHAEL PODLESAK

MRL-TR-92-39

OCTOBER 1993

DTIC
ELECTE
JAN 2 4 1994
S C D

94-01964

APPROVED

FOR PUBLIC RELEASE

© Commonwealth of Australia

MATERIALS RESEARCH LABORATORY

DSTO

Accesion For
NTIS CRA&I ☑
DTIC TAB ☐
Unannounced ☐
Justification
By
Distribution /
Availability Codes
Dist | Avail and / or Special
A-1

Breakwire Technique for Hypervelocity Measurements

Michael Podlesak

MRL Technical Report
MRL-TR-92-39

Abstract

An electrical breakwire technique for measuring the speed of hypervelocity projectiles is described and assessed, using Boomer, a large scale exploding foil flying plate generator. Two techniques were tested, a dual breakwire method and a single breakwire method. The dual breakwire method is the simpler of the two, but it was found to be less reliable than the single breakwire approach. With the single breakwire method, a reasonable approximation to the projectile's velocity-time-history can be obtained by conducting a series of experiments where a range of times of arrival of the flyer is measured as a function of the breakwire position only. However, accuracy of this technique depends on shot-to-shot consistency and the velocity versus time resolution is limited by the number of different positions of the projectile's trajectory at which the firings can be performed. Compared with other velocity measurement techniques, the breakwire method was found reasonably consistent and effective, in terms of simplicity, turnaround time, low cost and ability to operate within an environment containing high levels of electromagnetic noise in the radio-frequency and optical spectrum. Analysis of the breakwire data from Boomer experiments has indicated a possibility of improvement in the accuracy of the single breakwire technique through correlation of the time-of-break with variations in the Boomer-current waveform.

DSTO MATERIALS RESEARCH LABORATORY

94 1 21 172

Published by

DSTO Materials Research Laboratory
Cordite Avenue, Maribyrnong
Victoria, 3032 Australia

Telephone: (03) 246 8111
Fax: (03) 246 8999
© Commonwealth of Australia 1993
AR No. 008-223

APPROVED FOR PUBLIC RELEASE

Author

Michael Podlesak

Michael Podlesak obtained BSc(Hons) in Physics in 1980 and PhD in Physics, Acoustics, in 1986, at La Trobe University. After one year of postdoctoral work in acoustics, and one year of Physics teaching and research in the area of optical fibre application to sensing with the Department of Applied Physics at Footscray Institute of Technology, Dr Podlesak joined the Explosives Ordnance Division, MRL in 1988, to carry out experimental work in slapper detonator research and study shock wave phenomena in inert and energetic materials using electrically based launching methods. He is currently working in the Ship Structures and Materials Division on problems related to control of acoustic signatures of naval vessels.

Contents

1. INTRODUCTION 7

2. BACKGROUND 9
2.1 *The Dual Breakwire Method* 10
2.2 *The Single Breakwire Method* 10
2.3 *The Breakwire Failure Mechanism* 10

3. EXPERIMENTAL METHOD 11
3.1 *The Breakwire System* 11
3.2 *The Breakwire Sets* 13
3.3 *Apparatus* 14

4. EXPERIMENTAL RESULTS AND ANALYSIS 14
4.1 *Time of Arrival Measurements* 16
4.2 *Dual Breakwire Experiments* 21
4.3 *Single Breakwire Experiments* 25

5. EFFECTS OF FLYER-BREAKWIRE INTERACTION 33
5.1 *Physical Evidence of Flyer-Breakwire Interaction* 33
5.2 *Effect of Intrinsic Failure Delay Time* 34
5.3 *Effect of Shocked Air Layer* 35

6. ERROR ESTIMATES 36

7. ALTERNATIVE TIME-OF-ARRIVAL MEASUREMENTS 36

8. CONCLUSION 38

9. ACKNOWLEDGEMENTS 39

10. REFERENCES 39

APPENDIX 1 – *Boomer Current Waveform: Defining the Bridge-Burst Point* 42

APPENDIX 2 – *Shock Hugoniot Parameters for Copper and Polycarbonate* 43

Breakwire Technique for Hypervelocity Measurements

1. Introduction

After construction of the MRL Boomer rig [Podlesak *et al.* 1993], designed to produce hypervelocity flying plates for shock wave studies, initial calibrations were performed using an electrical breakwire method. The principle of Boomer operation is based on the propulsion of small plastic flying plates (flyers) to velocities of several km/s by exploding thin metal foils through a rapid electrical discharge.

The breakwire method described in this report is based on sets of twisted pairs of thin, enamelled, current carrying copper wires, placed in the flight path of a high velocity flyer plate (see schematic diagram in Fig. 1(a)). When the projectile impacts the wires, it breaks them and interrupts the electrical current flow. The sudden change in current is detected and recorded as time of arrival of the flyer plate. With two or more times of arrival recorded at successive breakwire positions, an estimate of the flyer velocity can be obtained.

Our use of the breakwire technique, while simple in concept, encountered complications, chiefly related to the intense electromagnetic noise generated during the Boomer rig firings. We found that some understanding of the flyer generation process is required in order to successfully interpret the breakwire signals. Some aspects of the wire breaking process were also found to affect the timing accuracy.

Two approaches to the flyer velocity measurement were investigated; a dual breakwire method and a single breakwire method. The first is based on obtaining an average velocity value from two wire breaks in one single experiment. The second relies on successive accumulation of single breakwire data from experiments identical in every aspect except for the variation of the breakwire position. We decided to adopt the second technique because it was found to give more reliable data and it can provide information on the flyer velocity profile with respect to time or flyer displacement.

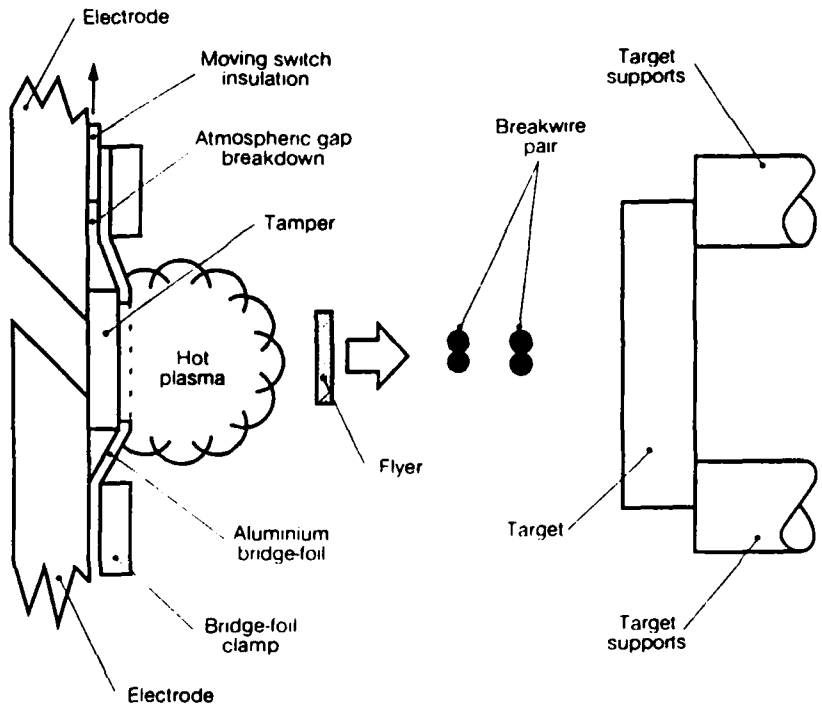

(a)

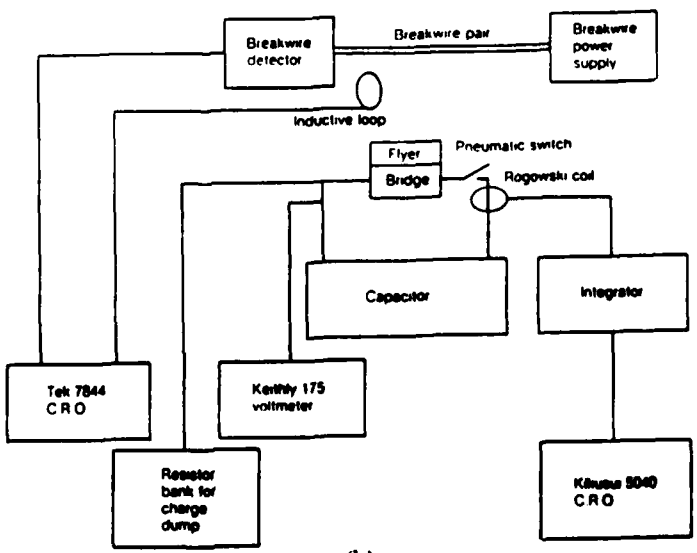

(b)

Figure 1: Schematic diagram of experimental apparatus (a) and measurement set-up (b).

The knowledge of flyer velocity-time-history from launch to impact provides a key to understanding the Boomer behaviour and helps to optimize the experimental set-up for maximum flyer velocity. The VISAR (Velocity Interferometer System for Any Reflector), for example, is well suited to provide such a velocity-time-history record (e.g. Barker and Hollenbach (1972), Stanton (1976) or Hatt (1991)). However, in this work, only an approximate estimate of the average velocity-time-history was obtained with an estimated error of about 20 to 30% in the neighbourhood of the flyer velocity maximum. The method we used has the advantage of simplicity and economy compared to methods such as the VISAR, however.

While the breakwire measurements obtained so far display limited accuracy, some of the data suggest that better accuracy could be attained through correlation with electrical current waveforms from the Boomer apparatus.

We considered several other methods of flyer velocity measurement such as high speed framing photography, flash x-ray radiography and laser Doppler interferometry. These were either not available to us at the time, or were judged to be impractical or doubtful in their effectiveness. Depending on the technique employed, difficulties were expected in the flyer velocity measurements on the MRL Boomer rig. The main difficulties are the following:

(i) strong electromagnetic radio-frequency interference,
(ii) strong broad-band optical emissions,
(iii) high temperature, high voltage plasma in close contact with the flyer and portions of the target,
(iv) small lateral cross-section of flyer projectile,
(v) high degree of flyer transparency to x-rays, and
(vi) short acceleration distances.

With the breakwire technique, we were able to either avoid or work within such limitations.

2. *Background*

The breakwire method is conceptually very simple and was used before the advent of optical beam interruption detectors. While the latter provide a generally superior alternative in many time-of-arrival or object detection applications, the problem of strong optical broad-band radiation and obscuration from the explosion by-products prevented us from using an optical-beam-interruption method (see also comments in Section 7).

In our treatment, we make a basic distinction between velocity estimates obtained from a single shot experiment (the dual breakwire method) and those obtained from cumulative experiments (the single breakwire method).

2.1 *The Dual Breakwire Method*

The velocity of a rectilinearly moving object can be estimated by measuring the time of its arrival, t_1 and t_2, at two closely spaced points x_1 and x_2, respectively. The estimated or average velocity is:

$$v = (x_2 - x_1) \quad / \quad (t_2 - t_1) \tag{1}$$

In the limit, as x_1 approaches x_2 (or t_1 approaches t_2), v becomes the instantaneous velocity of the object. Practical considerations of the breakwire method limit the minimum separation of the points x_1 and x_2 due to the spatial error (δx) and temporal error (δt). Also, we expected that the flying object may be affected by the breakwire. This turned out to be an important factor in the dual breakwire experiments and we discuss this in Sections 4 and 5.

2.2 *The Single Breakwire Method*

For a fixed set of launch parameters, which ensure a unique and specific trajectory of projectile motion, a range of (x, t) points is obtained from a series of single shot, single breakwire experiments. The data set (x_1, t_1), (x_2, t_2) ..... (x_n, t_n) .... thus generated may be fitted by a polynomial or some other curve fitting form. This is then differentiated with respect to time to obtain an approximate velocity-time-history curve. From this, one is able to characterize the projectile's velocity as a function of time or displacement. If some uncertainty exists in the shot-to-shot constancy of the flyer trajectory, then an average value of t_n can be obtained from several repeats of the same experiment (x_n, t_n).

2.3 *The Breakwire Failure Mechanism*

Accuracy of the breakwire method relies on a fast change in the electrical current flowing within the breakwire. The circuit used in our experiments is designed to detect time rates of change of current in the breakwire circuit rather than a change in its level which, as shown in the subsequent sections, is an important feature because of the presence of the ionized aluminium vapour from the exploded Boomer bridge foil.

The exact mode of mechanical failure of the breakwire when impacted by a hypervelocity projectile is not known, but we suspect that it is similar in fundamental aspects to that found for hypervelocity projectile impact on a thin metal sheet (see for example Kinslow (1970), Herrmann and Wilbeck (1986), Segletes and Zukas (1989), Holian and Holian (1989), Schulz *et al.* (1987) or Piekutowski (1990)). At high impact velocities, i.e. approximately 2 km/s and above, shock interaction of the projectile and target plays an important role and even though the target may be quite small, significant amount of damage can be inflicted on the projectile bulk and its surface. At low velocities (approximately 1 km/s or less) one is primarily concerned with momentum relations between the projectile and target (Piekutowski, 1990), and failure mechanisms such as adiabatic shear. Hence, when designing a breakwire velocity measurement system for hypervelocity projectiles (> 2 km/s), it is not only

necessary to consider overall momentum changes of the flyer and the effect this has on its velocity, but one also needs to be aware of the shock damage to the flyer plate caused by the breakwire impact.

Gehring (1970), and Hermann and Wilbeck (1986), show that the impact of a hypervelocity projectile on a thin metal sheet sets up shock waves within the projectile as well as the thin target. Intense rarefaction waves emanating from the unconstrained edges of the impact interface and the rear surface of the target are generated, which produce large tensile stresses within the target and cause it to fail and spall. In some instances, the projectile can also undergo disintegration to form a spray of microparticles or a cloud of vapour.

As explained by Hermann and Wilbeck (1986), since the shock compression process is dissipative, the temperature of the material on release to zero pressure is higher than the initial temperature. For strong shocks, generated in hypervelocity impacts, the residual temperatures may be sufficiently high to weaken, melt or even vaporize the released material.

We can infer from this work, and also the work of Schultz *et al.* (1987), the general principles that might apply to hypervelocity collisions between a flyer plate and breakwires. Firstly, as expected, target penetration is more rapid at higher projectile velocities and smaller target thicknesses, and penetration is more effective for projectiles with greater material density (which also increases the projectile's shock impedance). Secondly, the relative damage to the projectile is inversely proportional to the projectile-to-target thickness ratio. For small ratios such as 1:1 or 1:2, the projectile can suffer severe damage whereas for ratios such as 7:1 (equivalent to Boomer-flyer-plate to breakwire thickness ratio) the damage is expected to be less severe though not negligible. Results of multiplate impact modelling illustrate the change in projectile morphology through the first impact and how this affects the penetration of the second target plate. Clearly, inaccuracies could be expected to arise in the dual breakwire technique due to such an effect, particularly at higher velocities.

3. *Experimental Method*

A schematic representation of our measurement set-up is portrayed in Figure 1. Figure 1(a) shows the flyer launching assembly together with breakwires and a sample target with supports. Figure 1(b) shows the major components of the breakwire system and the associated measurement apparatus.

Because of the high voltages (3 to 10 kV) employed in the flyer generation process, the breakwire apparatus had to be electrically isolated to prevent stray discharges from damaging the measurement apparatus. This consideration dominated much of the practical design of the breakwire system.

3.1 The Breakwire System

The system, portrayed in Figure 2, consists of a low dc current source connected in series with a high frequency isolation transformer via a twisted pair of breakwires. Note that the dual breakwire method employs two of such systems. The 220 Ω series

resistors limit the drain on the current source, provided by a small 9 V battery, to about 40 mA. Miniature 50 Ω coaxial cables were used to connect the breakwires to a pair of rf shielding boxes containing the current source and the signal transformer, respectively. The signal transformer was constructed from an insulated torroidal ferrite core with single turn primary and secondary windings. These windings were further insulated from the core by wrapping 75 μm Kapton foil around the ferrite core, whose minor diameter was about 10 mm and major diameter about 50 mm. A 50 Ω RG U58 cable was connected to the secondary winding, but insulated from the shielding enclosure, to provide signal output for a recording device such as a storage oscilloscope or a transient waveform digitizer.

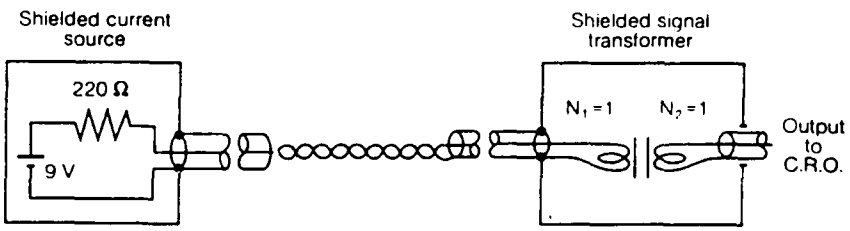

Figure 2: Schematic circuit diagram of the single breakwire system. The shielding enclosures are linked to a common reference. However, the output from the transformer is electrically decoupled from this common reference

The breakwire system was designed to minimize the effect of intense radio-frequency interference caused by Boomer current transients. However, a moderate amount of interference pick-up proved to have some advantages as discussed in Section 4. Noise generated by capacitive coupling between the Boomer rig and the breakwire circuit is insignificant compared to that caused by the inductive coupling since the breakwire circuit has low impedance and is current rather than voltage sensitive. It is quite conceivable that a small amount of resistive coupling between the Boomer and breakwire circuits could occur during the wire breaking process via the bridge-foil plasma, and should contribute to current changes in the breakwire circuit. This may also explain the excessive noise in some breakwire traces observed after the wire break (refer Section 4.1).

When the wire pair is broken by the projectile, a short voltage pulse is generated at the output of the isolation transformer, providing a timing mark for velocity estimation. This pulse represents approximately the first time derivative of the breakwire current and is therefore sensitive to current changes rather than complete interruption.

3.2 *The Breakwire Sets*

Each breakwire set was constructed from a twisted pair of enamelled copper wires, with outer diameter of 0.07 mm, and length of about 200 mm. Push-on type connectors were attached to each end of the pair to enable easy attachment to the connecting cables. The wires were mounted on a perspex base firmly attached to the base with adhesive tape. The breakwires were mounted under static tension, near breaking point, to ensure maximum positional accuracy at the time of break. Initially, the lateral separation of the wire supports was approximately 100 mm. Later, additional brass supports, shown in Figure 3, were added to reduce the free breakwire length to less than 50 mm. The distance between the breakwires and their displacement from the flyer plate starting position were measured within an accuracy of 0.5 mm. The initial position of the breakwires with respect to the flyer ranged from 2 mm to 30 mm, with the wires located to intercept the flyer at the centre of its impact face.

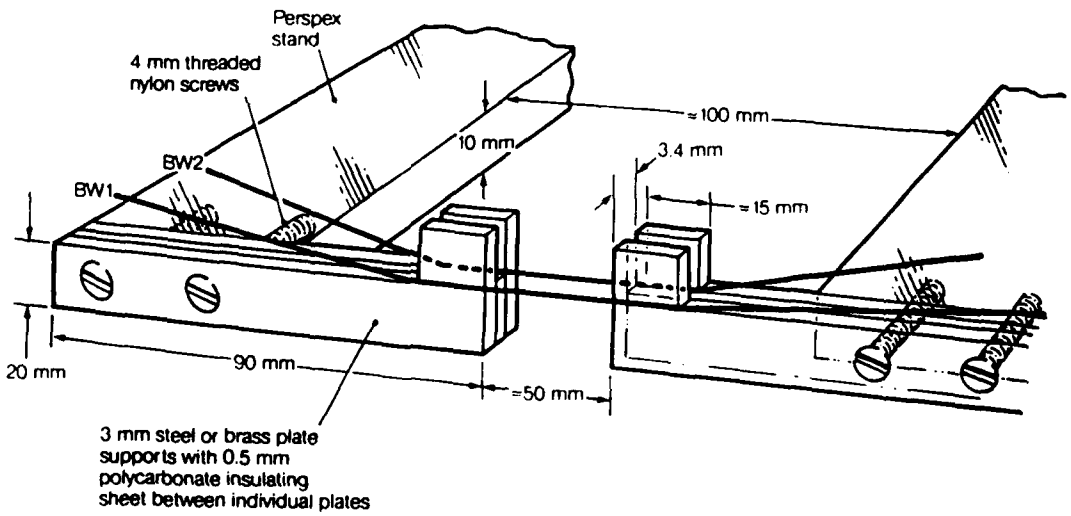

Figure 3: Representative diagram of the breakwire supports consisting of spaced L-shaped brass plates mounted on a Perspex base.

3.3 *Apparatus*

Referring to the general layout in Figure 2, the following apparatus was used:

(i) Boomer I (see Podlesak *et al.* 1993 for more detail): MRL large scale flying plate generator rig with maximum system energy rating of 10 kJ, at 10 kV, producing polycarbonate flyer plates with dimensions of 0.5 mm × 10 mm × 15 mm. Practical flyer velocities ranged between 1 and 5 km/s, as measured in the present work.

(ii) Current in the Boomer was measured via a Rogowski coil with passive integrator (Podlesak, 1990) and the signal recorded on a Kikusui 5040 digital storage oscilloscope. The oscilloscope's analogue bandwidth was 40 MHz and the maximum digitising rate was 20 Ms/s. The record length consisted of 512 data points.

(iii) The energy storage capacitor voltage was monitored by a Radio Spares high voltage 40 kV dc probe with input resistance of 1 GΩ and a voltage divider ratio 1000:1, with its output terminated in the 10 MΩ input of a Keithly 175 digital multimeter.

(iv) A Tektronix 7844 analogue dual beam oscilloscope with high intensity phosphor CRT screen was used to record the breakwire output signal in most of the experiments. The oscilloscope was configured with two 7A26, 1 MΩ input impedance and 200 MHz bandwidth vertical amplifier plug-ins and was operated in the single shot mode. The signal waveforms were recorded on a Tektronix C51 oscilloscope camera, using 3000 ASA black and white Polaroid film.

During the single breakwire shots, a 12 mm diameter inductive loop was placed on the breakwire stand to monitor the electromagnetic noise emission from Boomer. This signal was recorded on the second channel of the 7844 oscilloscope.

(v) In some shots the voltage across the Boomer bridge foil was measured with a Tektronix P6015 high voltage probe, with signal bandwidth of 0 to 75 MHz.

4. *Experimental Results and Analysis*

A complete set of data obtained from the 3 kV and 5 kV shots is presented in Tables 1 and 2, respectively. The experimental data of all breakwire measurements, excepting the second breakwire data in the 3 kV shots, are also given by Podlesak *et al.* (1993). In this report, we consider two example cases, namely the velocity determinations for 3 kV and 5 kV series of experiments.

Table 1: Data for 3 kV shots using the dual breakwire method

Shot No.	1st B-wire distance x_1 (mm)	2nd B-wire distance x_2 (mm)	1st B-wire time t_1 (μs)	2nd B-wire time t_2 (μs)	Average velocity v (km/s)
35	5.0	15.0	5.5	13.0	1.3
36	15.0	25.0	14.0	23.0	1.1
37	10.0	21.0	8.0	29.0	0.5
38	10.5	20.5	10.0	18.0	1.3
41	12.5	21.5	10.5	19.0	1.1
42	10.3	20.3	10.0	15.0	2.0
43	4.0	14.0	6.0	12.0	1.7
46	2.0	7.0	4.0	7.0	1.7
47	23.0	28.0	20.0	25.0	1.0
49	15.0	-	11.5	-	-
50	Rig Test				
51	5.0	7.0	5.0	8.0?	0.7
52	5.0	7.0	4.4	7.2	0.7
53	2.0	4.0	3.6	5.6	1.0
54	7.0	9.0	6.4	8.0	1.3
55	Camera mistrigger				
56	Breakwire traces illegible				
57*	4.0	7.4	4.3	7.6	1.0
58*	2.0	5.4	2.4	4.8	1.4
59*	6.0	9.4	7.6	9.2	2.1
60*	6.0	9.4	6.2	7.0	4.3
61*	8.0	11.4	9.6	11.0	2.4
62*	Premature discharge				
63*	8.0	11.4	8.0	10.0	1.7
64*	10.0	13.4	8.4	9.6	2.8
65*	12.0	15.4	9.2	10.4	2.8
66*	14.0	17.4	12.5	14.5	1.7
67*	16.0	19.4	11.0	12.5	2.3
68*	18.0	21.4	15.0	21.0	0.6
69*	Camera malfunction				
70*	20.0	23.4	16.0	20.0	0.9
71*	22.0	25.4	17.5	21.0	1.0
72-76	Boomer ringdown measurements				
77*	24.0	27.4	20.0	25.0	0.7
78*	26.0	29.4	18.5	22.5	0.9
79*	26.0	29.4	19.5	21.0	2.3
80*	26.0	29.4	18.0	20.0	1.7
81*	28.0	31.4	19.0	21.0	1.7

* New breakwire supports with brass plates used in all of these shots.

Table 2: Data for 5 kV shots using the single breakwire method

Shot No.	B-wire distance x_1 (mm)	B-wire time t_1 (μs)
95	5	3.3
96	5	1.9
97	*** No record ***	
98[1]	5	3.9
99-104	*** No record ***	
105[1]	30	13.5
106[1]	30	13.5
107[3]	30	13.0
108[2+]	30	14.0
109[1-]	15	6.5
110[2+]	15	6.0
111[1]	15	6.8
112[2+]	25	11.6
113[1]	25	10.6
114[1]	25	10.4
115[3]	20	8.0
116[1+]	20	8.0
117[2]	20	10.8

1 These shots displayed Type 1 current waveform.
2 These shots displayed Type 2 current waveform.
3 These shots displayed Type 3 current waveform.
\+ Denotes a larger than average value for a given current waveform type.
\- Denotes a smaller than average value for a given current waveform type

4.1 *Time of Arrival Measurements*

The breakwire signals were first recorded on two Kikisui 5040 digitising oscilloscopes (as described in 3.3 (ii)), triggered simultaneously by the Boomer current signal detected via the Rogowski coil. Later, the breakwire signals were recorded on a TEK 7844 oscilloscope. Figure 4 shows five traces synchronized in time and plotted with the same horizontal scale. The first three, (a), (b) and (c) represent the Boomer current and its respective first and second time derivatives obtained by successive numerical differentiations.

Breakwire 1 and 2 outputs, obtained from the photographic record in Figure 5(a), are shown in Figure 4(d) and (e). The traces indicate a temporal correlation between electromagnetic noise pick-up in the breakwires and the Boomer current transients, as shown by point (3) in the current and breakwire traces. This suggests that some inductive coupling exists between the Boomer current and the breakwire apparatus. The externally induced voltage signal in the breakwire loop is proportional to the first time derivative of the Boomer current which is further differentiated by the isolation

transformer because of the relatively high impedance of the transformer's output termination.[1]

Below, we discuss the correlation between the Boomer current waveform (including its first and second time derivatives) and the noise induced in the breakwires, and how this is used to interpret the experimental breakwire traces.

Five key features in the breakwire traces were identified and correlated with an equal number of distinct physical processes, explained below. These features are numbered and marked alongside the traces in Figure 4. In summary, feature (1) points to the onset of Boomer current and in all traces this represents the time of onset of all signals. Feature (2) relates to the burst of the bridge-foil in Boomer (see Appendix 1) and we define this point as the practical starting time of flyer plate acceleration. Feature (3) represents a random switching-like discharge frequently occurring after the bridge-foil burst and all five traces display this in one form or another at the same point in time (though the time of occurrence varies greatly from shot to shot). Features (4) and (5) represent the breaking of the first and second breakwire, respectively. The origin and significance of features (1) to (5) is explained below.

Feature (1) is induced by the onset of Boomer current and provides a valuable time reference mark. Feature (2), which we have chosen to be the time origin of the breakwire measurements, coincides with the first minimum in the first time derivative of Boomer current and is related to the time of burst of the bridge-foil (refer to Appendix 1 for a detailed explanation). Stanton (1976) has experimented with an exploding foil rig similar to Boomer and has shown, through his VISAR velocity records, that the flyer velocity increases slowly up to the point of bridge burst, after which it increases rapidly. He has shown that the flyer velocity at burst constitutes only some 5% or less of the maximum velocity. Therefore, one can neglect this relatively small value of flyer velocity at burst and set it conveniently to zero in the breakwire measurements, i.e. we use this mark as the time at which the flyer begins to move

Strictly speaking, according to the waveform of the second time derivative of Boomer current, shown in Figure 4(c), feature (2) identified in Figure 4(b) should appear as a zero crossing. However, the subsequent positive maximum is, as a rule, so close to this point that it may be equally chosen as the bridge-burst point without any significant error. Hence, we chose this point as the time origin in the flyer velocity-time-history.

[1] Simple tests of the isolation transformer with pulse stimuli have confirmed its band-pass limited nature and have shown its output characteristics to represent a differentiator within the bandwidth of our measurements.

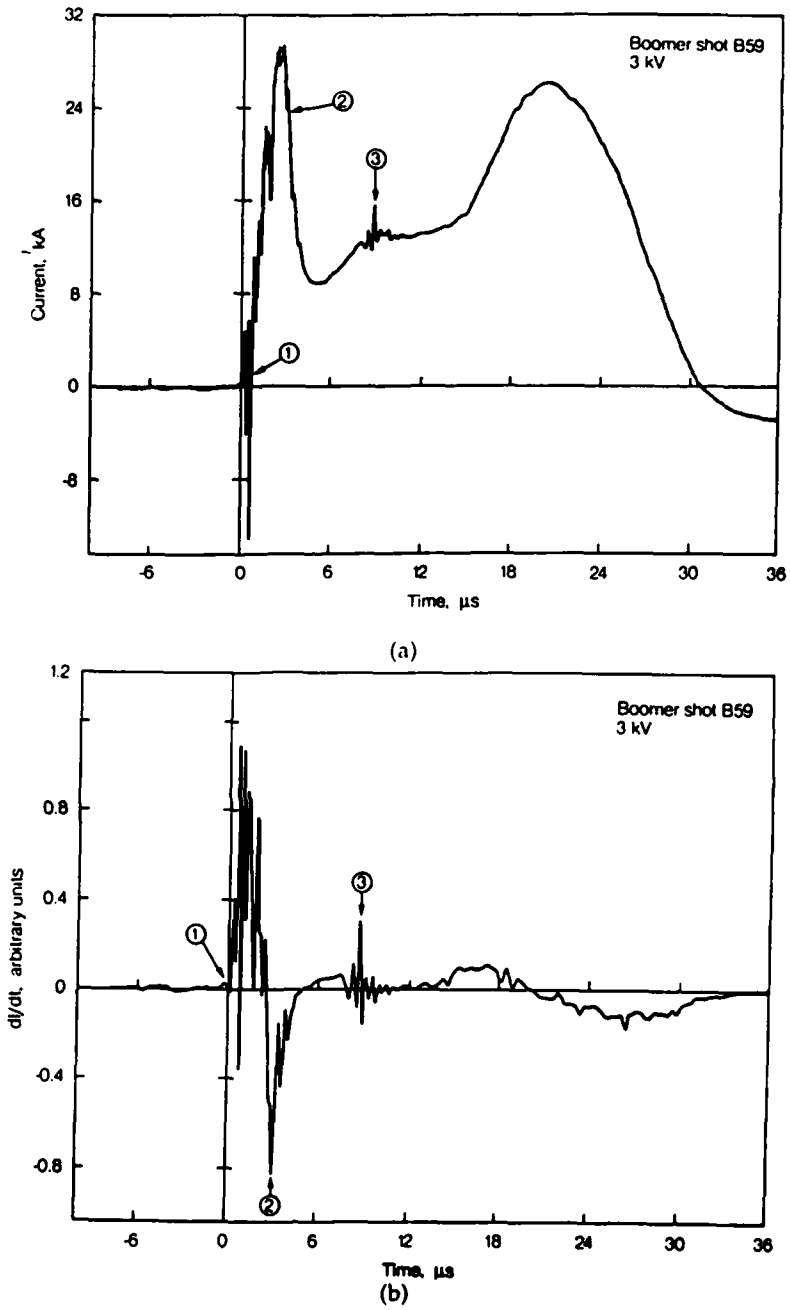

Figure 4: (a) Boomer I current waveform, Shot No. B59, fired at 3.0 kV. (b) The first time derivative of Boomer current in (a). (c) The second time derivative of Boomer current in (a). (d) The associated 1st breakwire waveform (digitized lower trace of Figure 5(a)). (e) The associated 2nd breakwire waveform (digitized upper trace of Figure 5(a)). The encircled numbers identify special features. (1) marks the time of onset of Boomer current, (2) the time of bridge burst, (3) the random discharge/switching noise, (4) the 1st wire break and (5) the second wire break.

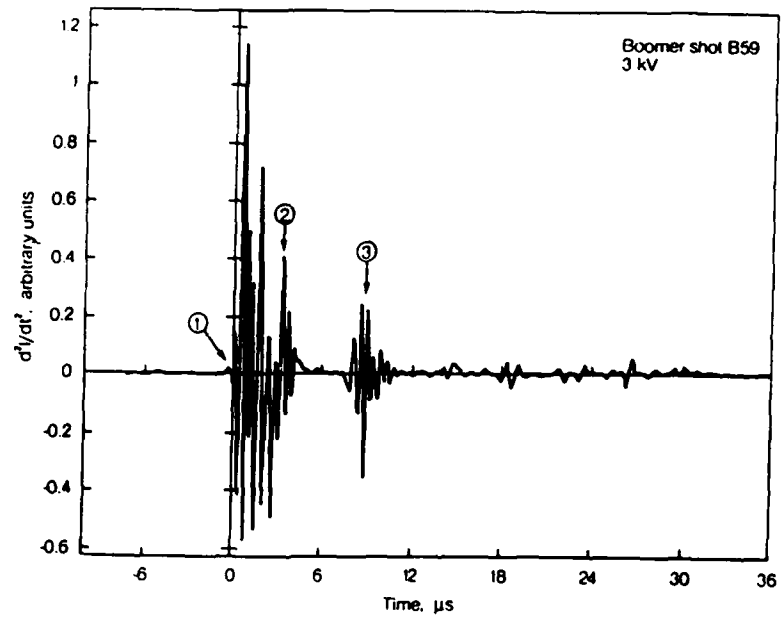

(c)

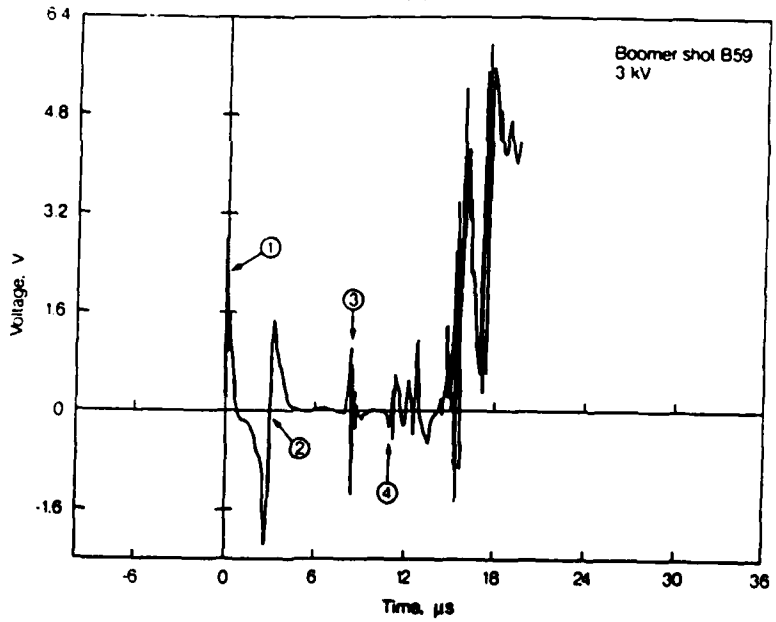

(d)

Figure 4 (Contd): (a) Boomer I current waveform, Shot No. B59, fired at 3.0 kV. (b) The first time derivative of Boomer current in (a). (c) The second time derivative of Boomer current in (a). (d) The associated 1st breakwire waveform (digitized lower trace of Figure 5(a)). (e) The associated 2nd breakwire waveform (digitized upper trace of Figure 5(a)). The encircled numbers identify special features. (1) marks the time of onset of Boomer current, (2) the time of bridge burst, (3) the random discharge/switching noise, (4) the 1st wire break and (5) the second wire break.

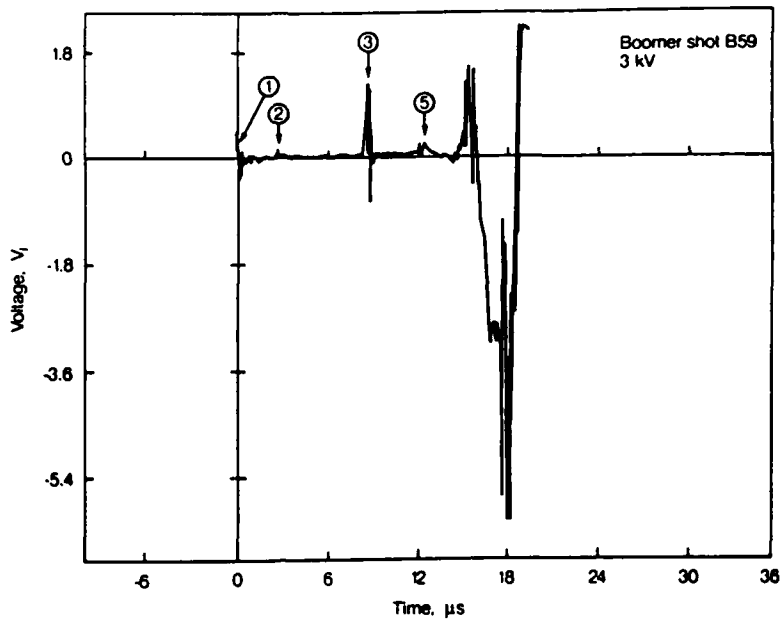

(e)

Figure 4 (Contd): (a) Boomer I current waveform, Shot No. B59, fired at 3.0 kV. (b) The first time derivative of Boomer current in (a). (c) The second time derivative of Boomer current in (a). (d) The associated 1st breakwire waveform (digitized lower trace of Figure 5(a)). (e) The associated 2nd breakwire waveform (digitized upper trace of Figure 5(a)). The encircled numbers identify special features. (1) marks the time of onset of Boomer current, (2) the time of bridge burst, (3) the random discharge/switching noise, (4) the 1st wire break and (5) the second wire break.

The high frequency noise generated by random discharges, identified in feature (3), can cause problems in the interpretation of breakwire signals. The best technique, so far, for distinguishing the breaking of the wire from such externally induced noise is by a combination of temporal and waveform correlation. Feature (3) indicated in all five traces of Figure 4 is a clear example of this. However, masking problems can arise if the electromagnetic noise occurs close to the wire break point, particularly in a dual breakwire measurement, where the noise may already be masked by the random signal fluctuations of the first wire break. This problem was readily overcome with the provision of a simple inductive pick-up loop monitor in the place of a beakwire set. The loop monitor traces (see for example Fig. 9) showed the occurrence of externally induced noise and the temporally correlated noise induced in the breakwire (a particularly distinct case is shown in Figure 9(c)). Hence actual wire break could be singled out most of the time as the first significant feature in the breakwire signal which was uncorrelated with the electromagnetic pick-up noise. In experiments, where the wire break appeared to be masked by the induced noise (e.g. Fig. 9(a)), the data could not be used. Frequently, waveform similarity in the inductively generated noise signals within the breakwire and the pick-up loop was

evident though mainly in terms of very high frequency oscillations, but not necessarily the waveform shape or envelope.

Many breakwire records display an intensely noisy signal at and after the breaking of the wire. This was more readily observed in experiments in which the breakwires were placed close to the flyer-bridge assembly, i.e. at a distance of 2 to 15 mm. For shots with breakwire distances of 20 to 30 mm, the noisy appearance was either much reduced or nonexistent (see for example Fig. 5, where the breakwire positions range 6 to 12 mm for Figs. 5(a) and (b) and 24 to 28 mm for Figs. 5(c) and (d)). We suspect that the noise originates from some form of resistive coupling between the breakwires and bridge-foil plasma current, but we have not been able to test this supposition.

4.2 *Dual Breakwire Experiments*

The dual breakwire technique was studied to obtain a flyer velocity estimate according to Eq. (1), with the wires placed in parallel on a plane surface, normal to the flyer trajectory. However, this technique was used only during the initial stages of breakwire experiments with some results collected during the 3 kV series of firings. It was found that the velocity estimates varied considerably, and at times, were unrealistic (e.g. shot 60 in Table 1). Inspection of the dual breakwire data revealed a wider spread in the times of flyer arrival for the second breakwire than for the first.

During the initial trials of the dual breakwire technique, the wires were positioned a considerable distance apart, i.e. about 10 mm. It was originally thought that the Boomer flyer plate would attain its maximum velocity within a few flyer thicknesses (≈ 2 mm, say) and then glide towards the target. Thus the spacing of 10 mm adopted was expected to give a reasonable estimate of the flyer velocity and reduce the contribution of position and time related uncertainties, δx and δt. However, this assumption was shown to be incorrect according to the results from the single breakwire experiments. In an attempt to improve the velocity estimate, a series of shots (No. 57 to 81, Table 1) was carried out with brass support plates spaced only 3.4 mm apart (see Fig. 2). These experiments yielded, contrary to our initial expectations, considerable scatter in the flyer velocity data and gave unrealistic values at times.

Figure 5 provides examples of records of breakwire traces from the dual breakwire experiments. Figures 5(a), (b), (c) and (d) represent the breakwire traces from shots 59, 63, 77 and 91 respectively, with corresponding first breakwire positions at 6.0, 8.0, 24.0 and 24.5 mm from the flyer's initial position.

In order to gain more information from the dual breakwire experiments, we applied the single breakwire method of analysis. Figure 6(a) represents a plot of breakwire position versus time-of-arrival of flyer for the first breakwire data from Table 1 (3 kV series) and Figure 6(b) those for the second breakwire. A third degree polynomial was used to fit the breakwire data which enabled inclusion of the starting point (0,0), but was of sufficiently low degree to filter out random fluctuations in the data. Comparison of Figure 6(a) with Figure 6(b) shows less scatter for the first breakwire data than for the second mainly in the 18 mm to 30 mm region. This is reflected in the difference between the least squares correlation coefficients of 0.981 and 0.935 from the first and second breakwire data fits, but the difference is not very large since the scatter in the 0 mm to 18 mm region is approximately the same for both the first and second breakwire data.

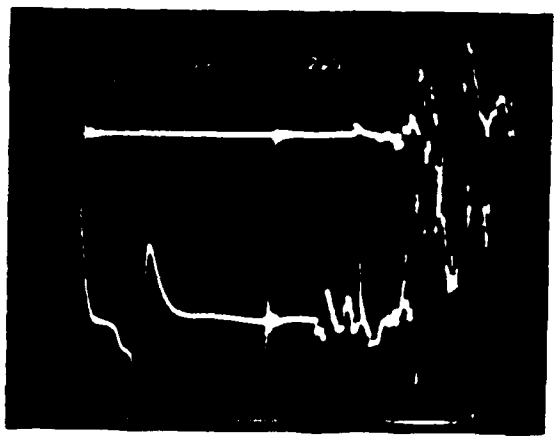

(a)

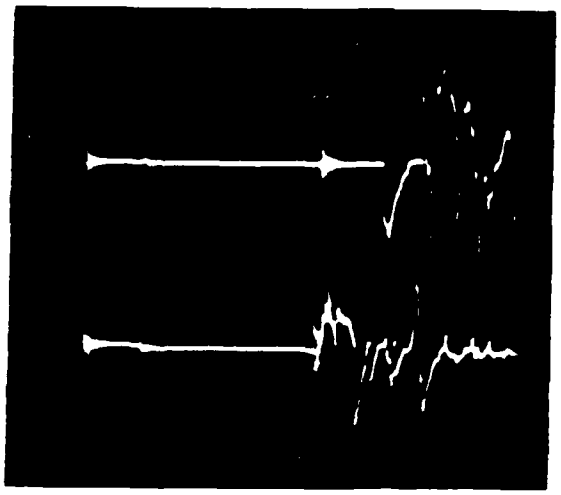

(b)

Figure 5: Examples of breakwire records, using the dual breakwire technique. In all oscilloscope records shown, the lower trace represents the 1st breakwire and the upper trace the 2nd breakwire. Records in parts (a) and (b) are scaled at 2 μs/division horizontally and 1 V/division vertically. Both records were obtained from 3 kV shots, No. 59 and 63 respectively. Records in parts (c) and (d) are scaled at 5 μs/division horizontally and 1 V/division vertically. Part (c) refers to shot No. 77 performed at 3 kV, whereas part (d) refers to shot No. 91 performed at 5 kV.

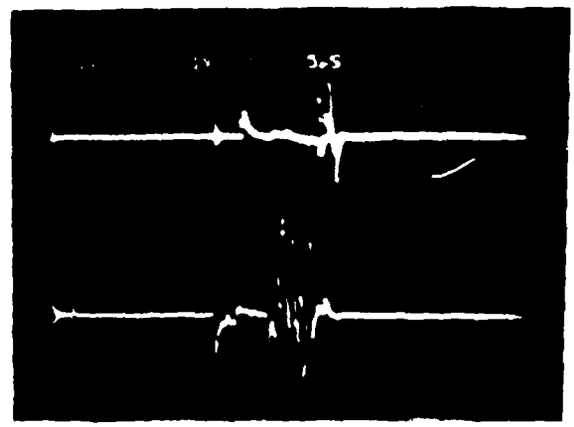

(c)

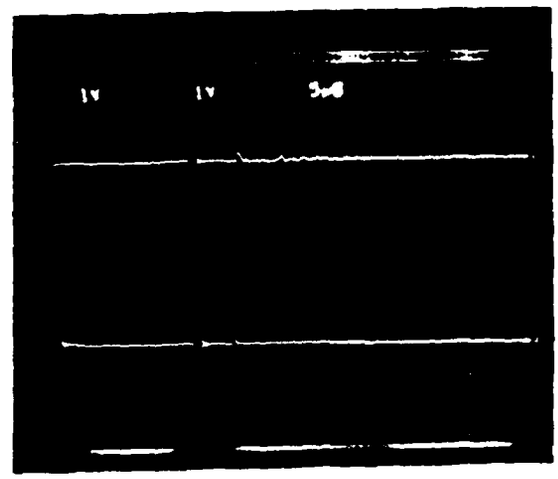

(d)

Figure 5 (Contd): Examples of breakwire records, using the dual breakwire technique. In all oscilloscope records shown, the lower trace represents the 1st breakwire and the upper trace the 2nd breakwire. Records in parts (a) and (b) are scaled at 2 μs/division horizontally and 1 V/division vertically. Both records were obtained from 3 kV shots, No. 59 and 63 respectively. Records in parts (c) and (d) are scaled at 5 μs/division horizontally and 1 V/division vertically. Part (c) refers to shot No. 77 performed at 3 kV, whereas part (d) refers to shot No. 91 performed at 5 kV.

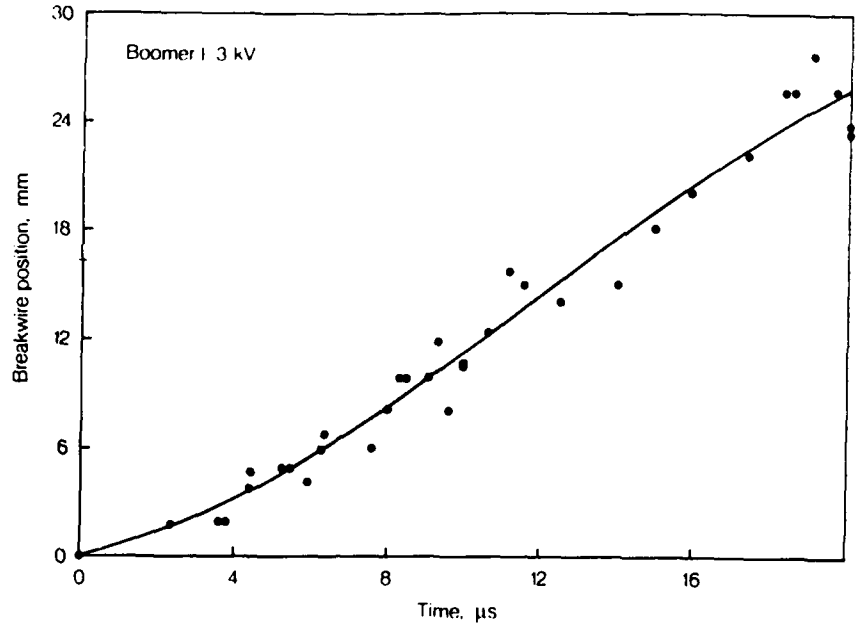

(a)

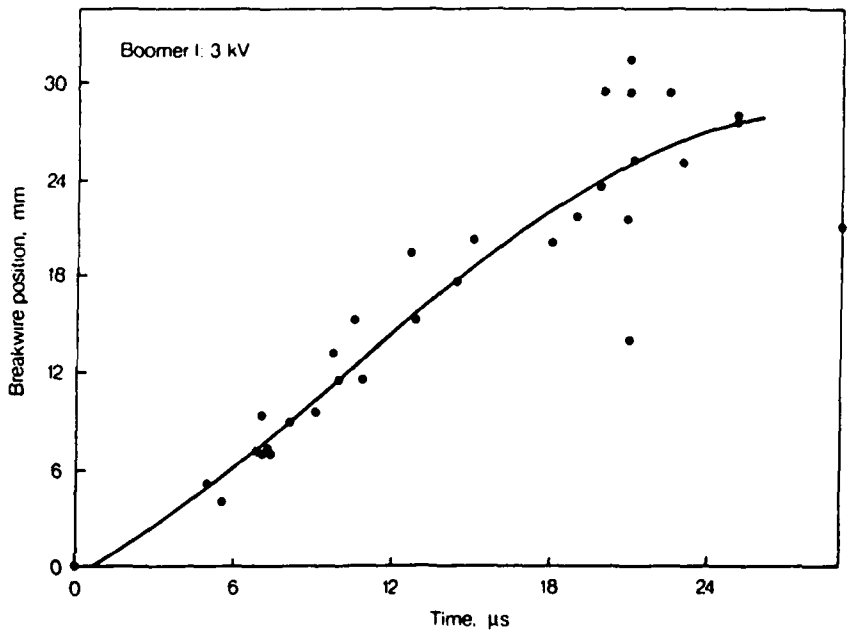

(b)

Figure 6: *Plot of breakwire position versus time of wire break for 1st breakwire (a) and 2nd breakwire (b). All data are from the 3 kV shot series, Table 1. The polynomial fitted to points in (a) is of the form* $x = -0.0026196t^3 + 0.09509t^2 + 0.4333t + 0.1295$*, with a correlation coefficient of 0.981. The polynomial fitted to data in (b) is of the form* $x = -0.0015074t^3 + 0.045428t^2 + 0.93114t - 0.58024$*, with a corelation coefficient of 0.935.*

The fitted polynomials were differentiated with respect to time to obtain an approximate velocity-time-history of the flyer, shown in Figure 7(a), as well as a velocity-position-history of the flyer, shown in Figure 7(b). Because of the uncertainty in the available data, the velocity curves are only approximate representations and errors are large near their ends. However, with good quality data and a sufficiently large number of points, better resolved and more accurate velocity curves could be generated.

For comparison, we show in Figure 8 direct velocity estimates from the 3 kV dual breakwire experiments superimposed over the velocity-flyer-position profile obtained from the first breakwire data. Here, the large scatter in the dual breakwire data is clearly evident.

4.3 Single Breakwire Experiments

The single breakwire method was adopted for the remainder of the Boomer characterization program because of better accuracy and consistency in comparison with the dual breakwire method. While some random shot-to-shot variation occurred, three reasonably consistent results were usually obtained in a set of three to five shots. A maximum spread of about 20% from the mean value was tolerated, though in most experiments much more consistent results were obtained with a spread of only a few percent.

Data from the 5 kV series of experiments were chosen to illustrate additional aspects of the single breakwire technique. Selected samples of photographic records of breakwire signals and inductive pick-up are portrayed in Figure 9, showing clearly the spiky noise from bridge burst transients. Table 2 contains the 5 kV series breakwire data which are also plotted in Figure 10(a). A third degree polynomial was fitted to all data points.

A careful study of the breakwire data revealed a high degree of consistency in the time-of-break readings for shots with nearly identical current waveforms. This suggests that much of the observed variation in the time of break for a given breakwire position is significantly influenced by shot-to-shot variation in the Boomer rig performance rather than some other type of random measurement error. Unfortunately, the Boomer current was not recorded successfully in all experiments, but for the 5 kV series, we found reasonably consistent current waveforms for shots 98, 105, 106, 111, 113, 114 and 116. The breakwire data from these are plotted and fitted with a third degree polynomial, as shown in Figure 10(b).

The polynomial curves from Figure 10 were used to generate the flyer velocity profiles as a function of time and position (see Fig. 11). In both Figures 11(a) and (b), the solid line is derived from the constant current waveform (CCW) — a subset of the 5 kV data as shown in Figure 10(b) — and the dashed line refers to that derived from the entire 5 kV data set.

The current waveforms associated with the CCW series were classed within three basic types, shown in Figure 12. The main differences between these types arise from the post-burst current characteristics within a time interval of about 6 to 17 μs after bridge burst. Note that the time origin was deliberately chosen at the approximate time of bridge burst in order to provide a reference point to which the breakwire times in Table 2 could be related. The CCW data, plotted in Figure 10(b), are associated with the current waveform of type 1.

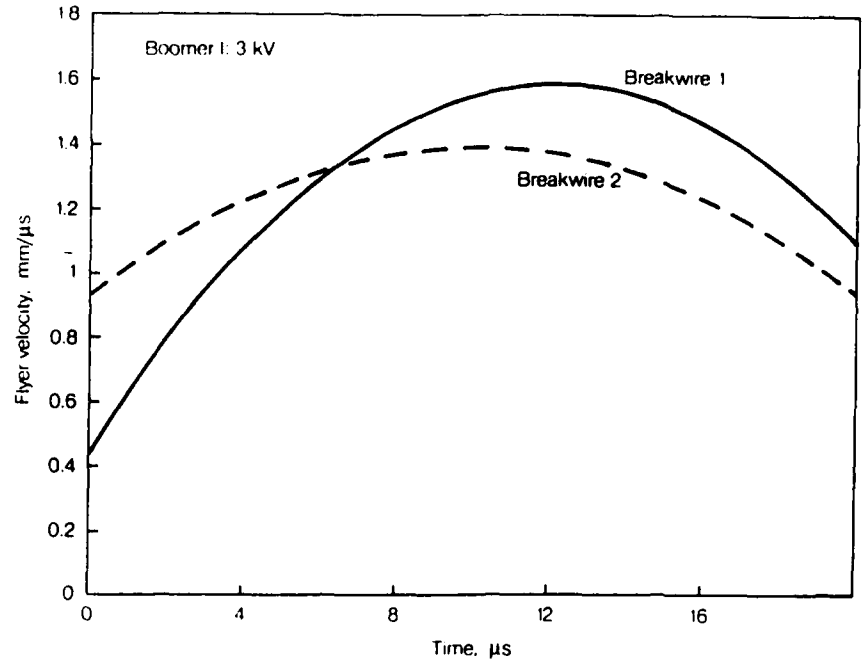

(a)

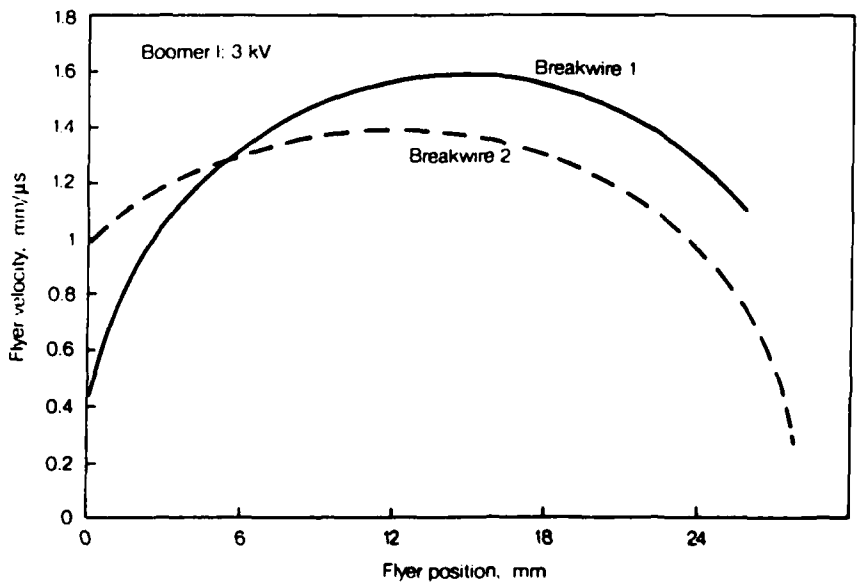

(b)

Figure 7: *(a) Approximate flyer velocity profiles as a function of time, for 3 kV firings. Solid line represents velocity profile obtained from polynomial fit of 1st breakwire data in Figure 6(a) and the dashed line represents the velocity profile obtained from polynomial fit of 2nd breakwire data in Figure 6(b).*

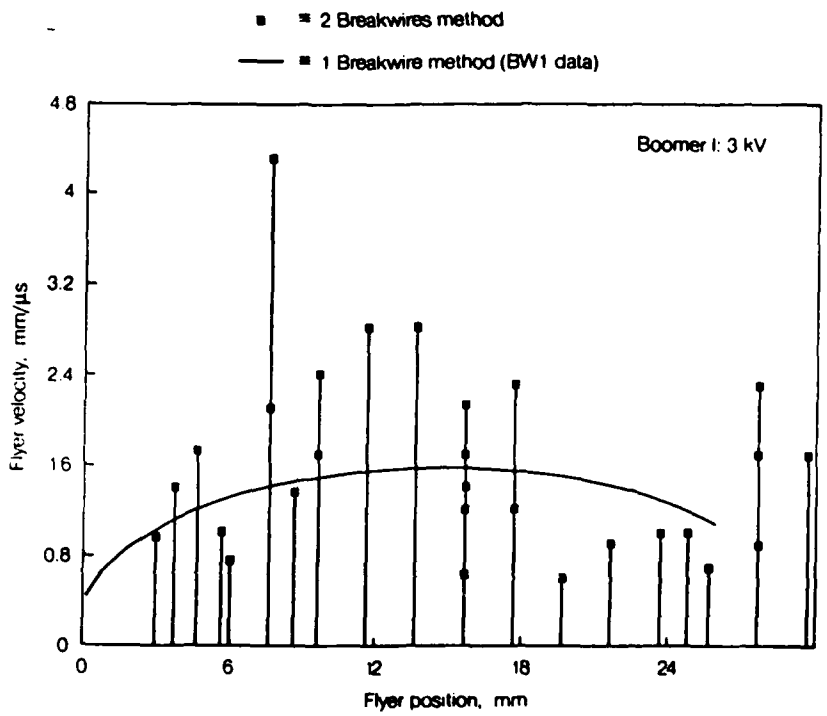

Figure 8: Plot of flyer velocity versus flyer position for 3 kV firings. Solid line represents the velocity profile from polynomial fit to the 1st breakwire data as in Figure 7(b). The individual points marked by open squares are those obtained via the dual breakwire method, with interwire spacing of 3.4 mm. The points are plotted at the median position.

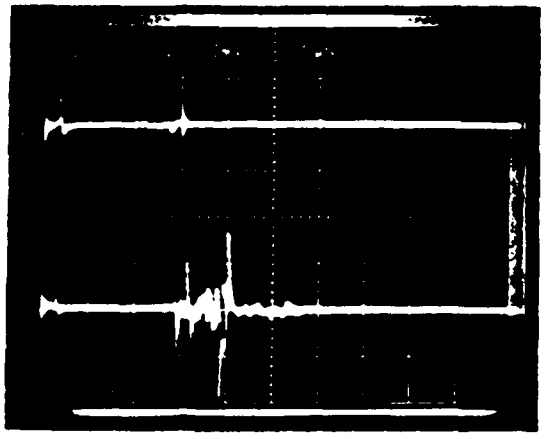

(a)

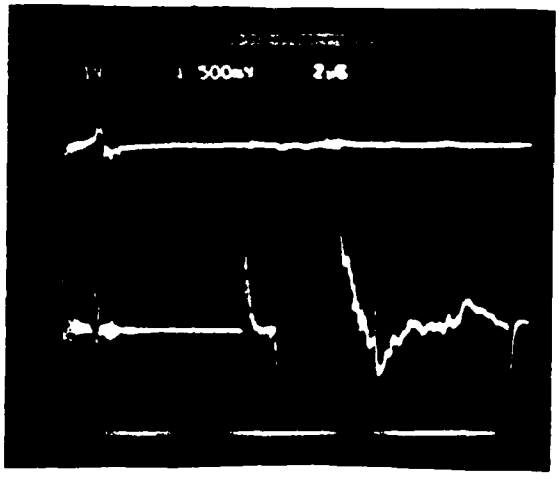

(b)

Figure 9: Examples of breakwire records from the 5 kV shot series, Table 2. The upper trace represents the inductive loop output, with vertical scale set to 1 V/division, and the lower trace gives the breakwire system output with vertical scale of 500 mV/division. Record (a) refers to shot No. 108, with horizontal scale set to 5 μs/division, record (b) refers to shot No. 110, with horizontal scale set to 2 μs/division and record (c) refers to shot No. 112, with horizontal scale set to 2 μs/division. The bridge-burst spike, noted as feature (2) in Figure 4, is clearly evident near the beginning of each record.

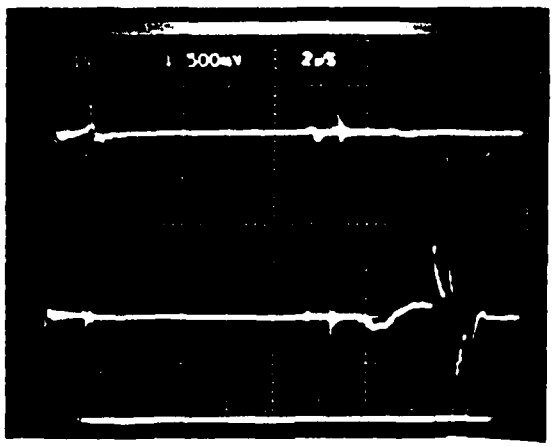

(c)

Figure 9 (Contd): Examples of breakwire records from the 5 kV shot series, Table 2. The upper trace represents the inductive loop output, with vertical scale set to 1 V/division, and the lower trace gives the breakwire system output with vertical scale of 500 mV/division. Record (a) refers to shot No. 108, with horizontal scale set to 5 μs/division, record (b) refers to shot No. 110, with horizontal scale set to 2 μs/division and record (c) refers to shot No. 112, with horizontal scale set to 2 μs/division. The bridge-burst spike, noted as feature (2) in Figure 4, is clearly evident near the beginning of each record.

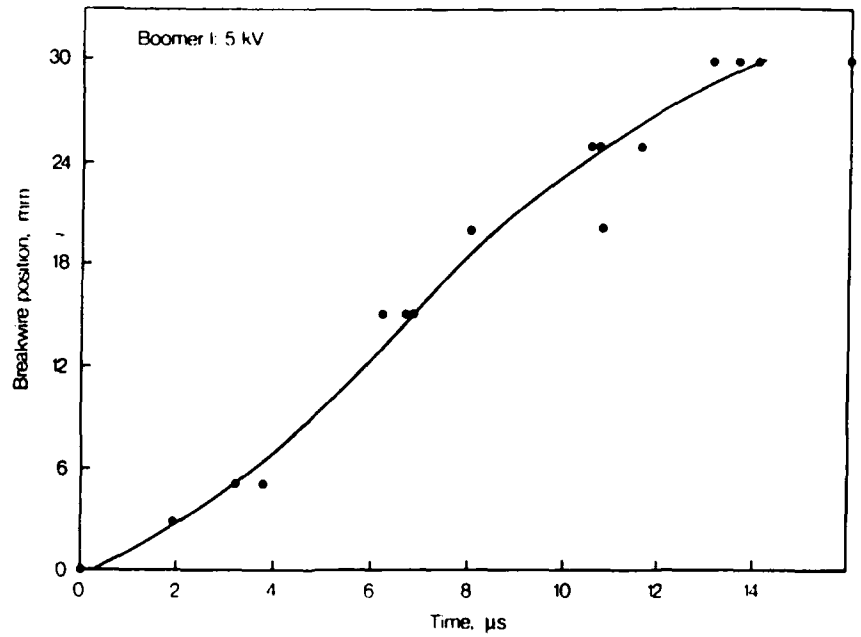

(a)

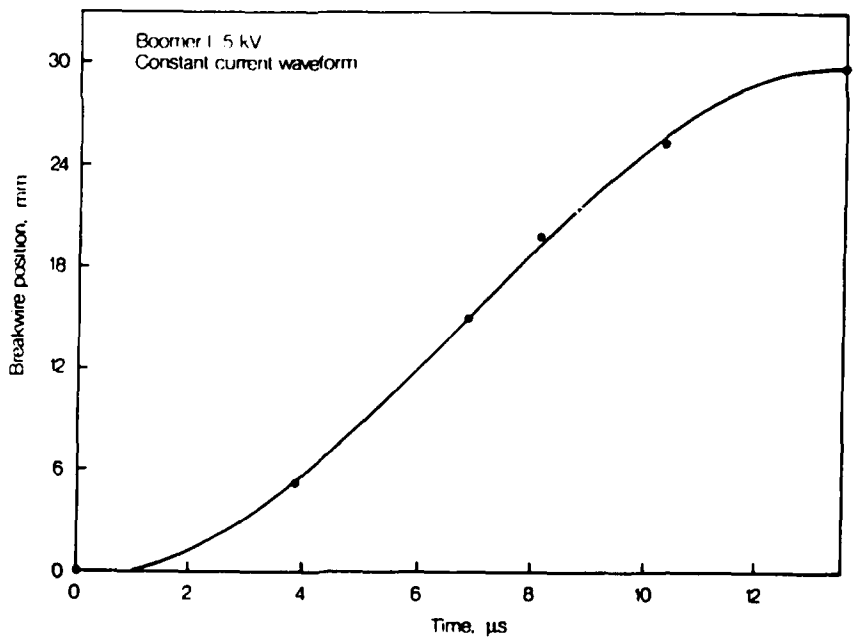

(b)

Figure 10: Plot of breakwire position versus time of wire break for all 5 kV breakwire data, Table 2, (a) and breakwire data with constant Boomer current waveform (b). The polynomial fitted to points in (a) is of the form $x = 0.00061272t^3 - 0.026065t^2 + 0.069396t + 0.2489$, *with a correlation coefficient of 0.980. The polynomial fitted to data in (b) is of the form* $x = 0.0010522t^3 - 0.04778t^2 + 0.93733t - 0.087163$, *with a correlation coefficient of 0.999.*

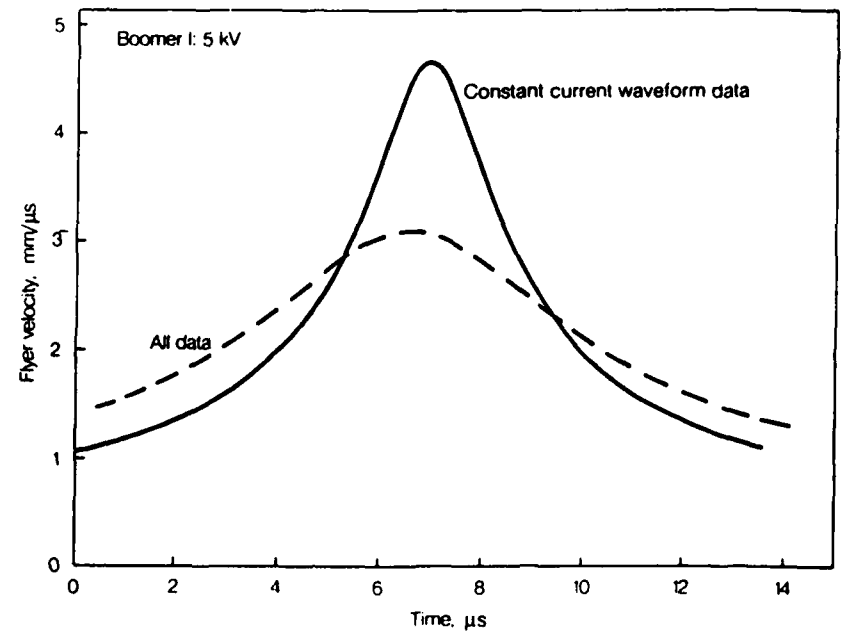

(a)

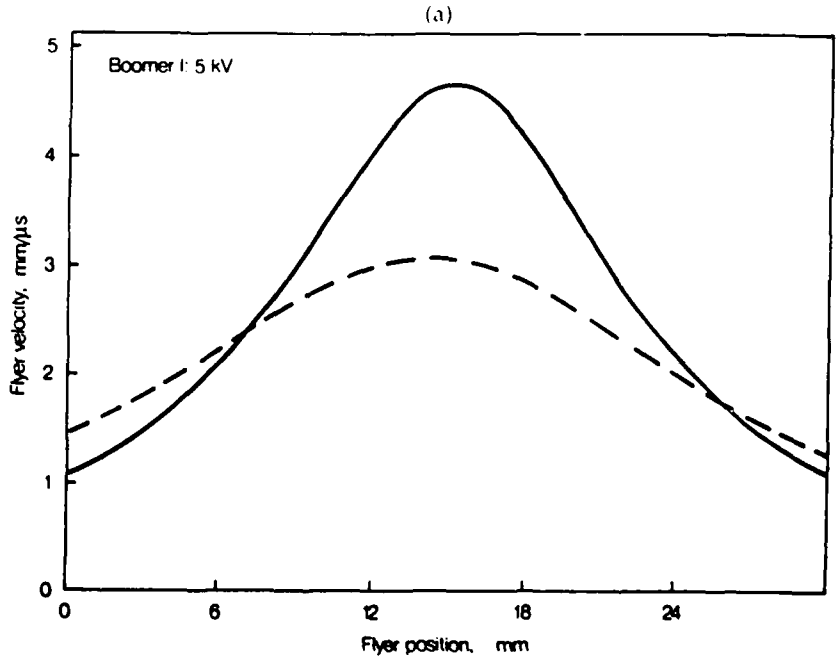

(b)

Figure 11: *(a) Approximate flyer velocity profiles as a function of time, for 5 kV firings. Dashed line represents velocity profile obtained from polynomial fit of all breakwire data in Figure 10(a) and the solid line represents the velocity profile obtained from polynomial fit of breakwire data in Figure 10(b), pertaining to the constant current waveform data subset. (b) Velocity profiles as in (a) but plotted as a function of the flyer position.*

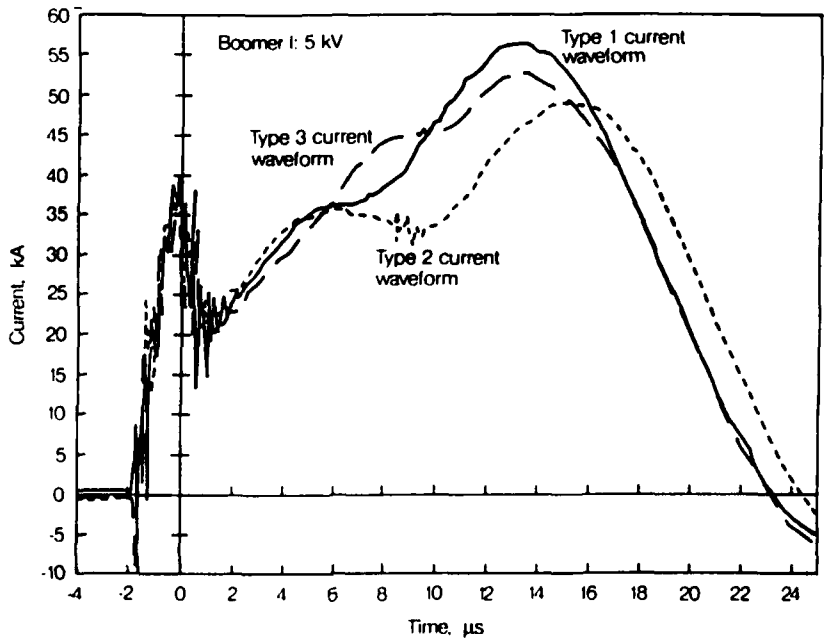

Figure 12: Three examples of the main types of current waveforms recorded in the 5 kV shot series. Solid line represents Type 1, fine dashed line Type 2 and coarse dashed line Type 3. The time origin was translated to the expected point of bridge burst for ease of time correlation with breakwire data.

In Figure 11, we see that the estimated peak velocity derived from the CCW data is about 50% higher than that derived from the whole 5 kV data set. However, while insufficient data is available in the CCW series to substantiate this dramatic difference, the increase in the maximum velocity estimate suggests that the CCW set with current waveform of type 1 yields better than average performance. Inspection of the time to break data in Table 2, reveals that between various current waveform types, increases in the levels of post-burst current result in earlier times of break. We also find that the times of break are remarkably consistent, provided that the current waveform is the same within a given measurement interval.

These findings suggest that additional energy is imparted to the flyer during the post-burst epoch and that it is strongly dependent on the post-burst current level.

Some investigators, e.g. Chau *et al.* (1980), claim that the Lorentz force (the cross product of current density and magnetic field intensity vectors) adds a significant contribution to flyer acceleration by exerting a force on the plasma behind the flyer. Therefore, higher post-burst currents ought to result in higher Lorentz force contribution to flyer plate acceleration.

We have made conservative estimates of the Lorentz force contribution and find that it does not exceed 10% of the total force on the flyer plate, which would result in only a 5% increase in the maximum flyer velocity. We suspect that additional Joule heating of the vaporized bridge plasma is more likely to provide a greater contribution to flyer velocity variations than the Lorentz force.

By inspecting the current waveform types in Figure 12, at the point of wire break, one can make a qualitative estimate of the cumulative current contribution towards the flyer acceleration. For example, with all three waveform types, the wire break times up to 6 μs should be nearly the same, since the current waveforms are also nearly identical up to this point. A comparison check of values in Table 2 for the 5 mm position is not possible because of misssing current waveform records for shots 95 and 96. However, for the 15 mm position, the breakwire times are similar for the two waveform types present, as expected. At the 20 mm position, the current waveforms begin to deviate from one another, though the Type 1 waveform recorded for shot 116 was greater in magnitude than that displayed in Figure 12. This accounts for the equal wire-break times with Type 1 and Type 3 waveforms while for the Type 2, the wire-break time falls significantly behind the other two as expected from the lower current level. The order of readings continues to be predictable at the 25 mm position. However, at 30 mm, the same reasoning applies, but because of a stronger Type 2 waveform (shot 108), the difference between the wire break times have virtually vanished.

5. *Effects of Flyer-Breakwire Interaction*

5.1 Physical Evidence of Flyer-Breakwire Interaction

As stated in Section 2.3, the breakwire failure mechanism is likely to consist of a mixture of adiabatic shear and spall due to shock loading arising from the flyer-breakwire interaction. Shock effects are expected to become increasingly important as flyer velocity increases (Schulz *et al.*, 1987).

Inspection of the breakwire remains from a number of experiments revealed that only the portion impacted by the flyer was severed and destroyed. The only visible remains of the impacted breakwire section were found embedded in the target as loose microscopic fragments. With the aid of a 20× optical microscope incorporating a 0.1 mm/division graticule, dimensions of the fragments viewed under the microscope ranged from 0.5 mm down to about 0.01 mm. This suggests that the impacted section of the breakwire was considerably fragmented.

Further evidence of the flyer-breakwire interaction was provided by the shape of the flyer imprints in the polycarbonate targets. 10 mm thick polycarbonate targets were used in most of the experiments and these show a definite (25 to 30 mm) × (12 to 15 mm) flat imprint due to the flyer plate, with an approximately 1 mm to 2 mm wide groove in the centre which roughly divided the overall flyer plate impression into two halves. This suggests that the flyer was either cut by the impact upon the breakwire or at least severely deformed in the region of breakwire impact. Because of this strong interaction between the flyer and the breakwire, the breakwire technique is not suitable as a direct projectile-velocity monitor except in experiments using very large surface area flyers (e.g. 50 mm × 50 mm), where some of the impact surface integrity could be sacrificed for velocity measurement purposes.

It should be noted that the intact portions of the breakwire end-tails appeared slightly charred over a length of 10 mm to 20 mm from the point of break, and upon inspection under a 100× magnification optical microscope, showed rounded conical tips with a taper of approximately 30°. Some breakwire end tips displayed a burnished surface and even secondary necking. Generally, the wire surface was eroded over a length of 2 mm to 3 mm from the tip end. Because of a 100 μs long immersion of the wires in the hot and high velocity plasma gas from the bridge-foil burst, and some evidence of multiple failure along the impacted wire length, we cannot expect the breakwire end-tails to provide detailed evidence of the wire failure mode critical to the detected electrical signal.

5.2 *Effect of Intrinsic Failure Delay Time*

The breakwire failure process has a finite response time which will introduce a delay into the time of break measurement. This may lead to erroneous estimates of the flyer velocity if the failure process is significantly flyer-velocity dependent. Other delays such as those due to signal propagation are negligible with respect to overall measurement uncertainties.

Without direct experimental evidence, such as high speed flash x-ray radiography or comparison against other time-of-arrival detectors with known characteristics, it is difficult to give a close estimate of the intrinsic failure delay time for the breakwire technique. At the lower end of the velocity range (≈ 1 km/s), shock effects are not expected to be pronounced, but the breakwire will be strained at high enough rate at the flyer edge so that the wire will undergo adiabatic shear.

Referring to the modelled examples by Schulz *et al.* (1987), we can expect significant localized fragmentation of the breakwire once the flyer has progressed five to seven wire diameters after the initial impact. This represents about 350 to 500 ns delay at flyer velocity of 1 km/s, and about 200 ns at 2.5 km/s. At velocities of the order of 5 km/s, the inferred 100 ns delay may be shorter since increased shock interaction between the flyer and the breakwire gives rise to greater and faster fragmentation through impact induced spallation and possibly some vaporization. The breakwire sections consisting of fragmented solid, liquid and partly vaporized copper will not necessarily be in highly ionized state and would therefore contribute to a sudden increase in the breakwire resistance. However, presence of the bridge-foil plasma near the flyer edges could possibly act against such a resistance increase.

The problem of wire and bridge-foil plasma interaction has not been clarified, though evidence from high speed photography in the work of Ryan (1993) has shown the expected blow-by effect of the bridge-foil gas. Hence, the gas impinges on the

breakwire ahead of the flyer, but since Ryan did not use the breakwire technique in his experiments the mechanical effect of the plasma on the breakwire failure process is not known. Electrically, the plasma can provide a conducting path, as mentioned above, and once the twisted breakwire pair is broken the plasma will tend to shunt the current supplied by the 9 V cell battery. Therefore a current change in the breakwire circuit is expected, whether induced by an open circuit condition or a plasma shunt, resulting in a corresponding voltage pulse at the output of the breakwire detector.

Using flyer displacement of seven wire diameters as the distance travelled by the flyer from impact to breakwire failure, we introduce an almost constant displacement error of approximately 0.5 mm. Such an error will distort the flyer velocity profile mainly at the initial stages of acceleration, when it is high, but will have a comparatively minor effect in regions of low acceleration, i.e. near the flyer velocity maximum, as explained in Section 6.

5.3 *Effect of Shocked Air Layer*

Since all of our experiments were performed under normal atmospheric conditions, a thin layer of shocked air will be generated ahead of the flyer plate. We expect some interaction between the shocked air layer and the breakwires, though it is not obvious whether this leads to premature breaking. Some estimate of the extent of the shocked air layer can be made from the shadowgraph of Rashleigh and Marshall (1978), which shows a layer of shocked air approximately 0.5 mm thick in front of a 5 km/s fast cubical macro-particle. The front surface of the macro-particle and the Boomer flyer plate are both flat and of comparable size. Hence, we expect a similar layer of shocked air to form in front of the Boomer flyer as shown for the macro-particle, but with greater thickness[2] than 0.5 mm for speeds less than 5 km/s.

Since the Boomer flyer reaches supersonic velocities (Mach 3 to 15), the density of the shocked air layer ahead of the flyer is expected to be about a factor of five to six higher than that of the unshocked air (Freedman and Greene, 1972). This density value is still about three orders of magnitude lower than the density of the copper breakwires and two orders of magnitude lower than the density of the polycarbonate flyer (refer Appendix 2). Even though the width of the shocked air layer is probably of the order of 1 or 2 mm for flyer velocities 2 to 3 km/s, the shock impedance mismatch between the shocked air and the breakwire, which is strongly governed by material densities, will be too great and result in relatively weak shock interactions. Hence, we conclude that the effect of the shocked air layer is unlikely to make a significant contribution to the wire breaking process, though if it did, it would probably help to negate the positional offset error due to the intrinsic failure delay time.

[2]. High speed photography in the work of Ryan (1993) has revealed approximately 1 mm to 2 mm thick layer of shocked air in front of the Boomer flyer for flyer speeds in the range of 1 km/s to 2 km/s.

6. *Error Estimates*

The error in the flyer velocity estimate depends mainly on measurement uncertainties, variation in Boomer performance and the number and distribution of data points used to generate the flyer velocity profile. Some errors could arise from misinterpretation of the breakwire records, but the contribution is expected to be small since dubious records are disallowed.

Reading error estimates are: breakwire position measurement (≈ 0.25 mm), wire break time measurement (± 0.2 μs) for records taken at sweep rate of 2 μs/div., and (± 0.5 μs) for records taken at sweep rate of 5 μs/div. These errors are mainly judged by the resolution of the measurement or recording apparatus. Errors arising from the interpretation of the wire break onset can be greater than simple reading errors, and depend on the skills of the interpreter. Interpretation errors can be reduced or eliminated by rejection of dubious or inconsistent results.

We estimate that for breakwire measurements performed near the point of maximum flyer velocity, the reading errors related to position (δx) and time (δt) range 5% to 10%. This results in a cumulative reading error of 10% to 20%.

The breakwire measurement errors are difficult to judge without some form of experimental verification using other well understood methods of measurement, e.g. flash x-ray radiography, VISAR, or time-of-arrival pin gauges (piezoelectric crystal or electrical contact type). However, the error in the flyer position due to intrinsic delay time, though significant in an absolute sense, is not expected to be important for flyer velocity determinations in the vicinity of the velocity maximum, where flyer acceleration levels are low. We assume that the intrinsic delay time will be almost constant for small variations in flyer velocity and therefore vanish after differentiation. The fact that the CCW shots give consistent results would imply that for a given flyer velocity, the intrinsic failure delay time is constant within the limits of experimental uncertainty. Only in the regions of large accelerations is this error likely to vary significantly and cannot be easily dismissed.

The estimated level of uncertainty in the maximum flyer velocity determination is of the order of 30%, taking into account reading error, scatter and in some cases paucity of breakwire data. A higher error level is expected for velocity estimates in the 7 and 9 kV series of experiments (Podlesak *et al.*, 1993), because of fewer available data points. In Section 4.3 we have shown the possibility of improving the accuracy of the flyer velocity determinations for Boomer experiments by using constant current waveform data.

7. *Alternative Time-of-Arrival Measurements*

In this section we discuss some of the other available methods of time-of-arrival measurement, where continuous velocity monitors, such as the VISAR, are either not available or cannot be readily applied.

A common technique for time-of-arrival measurement used in shock wave studies is based on pin detectors. These detectors are pin shaped and produce an electrical pulse upon impact. Two distinct types exist, one based on making an electrical contact and the other on generating a voltage pulse from a piezo-crystal element. We have attempted to use the latter, but unsuccessfully so far, due to electrical ground

isolation problems arising from contact between the Boomer bridge-foil plasma and the pin. The response time of such detectors is known to be in the submicrosecond region.

An optical breakfibre method was investigated by Szajman *et al.* (1989), but the results have not yet been validated by other proven methods, though the method shows considerable potential. The technique consists of mounting 125/50 μm multimode fibres on a support, in a similar manner as the breakfibres. The fibres are connecfed to optoelectrical converters, which respond to the Boomer bridge-foil self-light entering the optical fibres once they are broken. Some of the results obtained for 5 kV firings are not grossly inconsistent with the breakwire measurements, but could not be accurately compared because of random variations in the Boomer rig performance. The immediate benefit gained by this method was the absence of radio-frequency interference in the optical signals, though a small amount was picked-up through the power supply of the opto-electronic converter.

Using the optical breakfibre method, it should be possible to detect flyer impact when the fibre is severely deformed prior to complete mechanical failure. This may explain the observations made in some experiments, where low order precursive signals appeared prior to the main fibre failure.

In all breakfibre experiments, the dual breakfibre method was used. The recorded breakfibre signal onset was on many occasions very sharp with rise times less than 100 ns. However, the break times for the second fibre often varied in an unpredictable fashion and may have been affected by fragments from the first fibre-flyer interaction. An example of a breakfibre record is shown in Figure 13, where the high frequency noise is due to electromagnetic pick-up from the Boomer current transients.

The passive optical fibre method (Szajman *et al.*, 1989) showed much promise, particularly when applied to the medium scale flying plate generator (Ryan *et al.*, 1989). Optical fibres were embedded in a barrel, through which a thin polyimide flyer was projected using an electrically exploded bridge-foil. The foil vapour was confined behind the flyer and the passage of the flyer past the fibre endings registered a fast-rising optical pulse. Hence, as for the breakwire method, time of flyer arrival versus position could be obtained, but in this case the mechanical interference of the fibres with the flyer was eliminated. Preliminary trials, using a 10 mm thick barrel with a 12 mm diameter, were performed on the Boomer rig with encouraging results. However, some difficulties were encountered with foil vapour confinement at the base of the barrel which may have resulted in lower flyer velocities (at 5 kV, velocities of the order of 3 km/s were measured[3]). This technique was applied unsuccessfully to shots without a barrel, which gave poor time-of-arrival resolution and probably suffered inaccuracies arising from unrestrained blowby of the glowing bridge-foil gas.

In another set of trials, Ryan (1993) employed a 15 mW Helium-Neon laser to conduct optical breakbeam experiments on a Boomer rig, using 1 nm narrow bandwidth laser-line interference filters. The problem of the intense self-light from the vaporized aluminium bridge-foil was successfully overcome, but with the aid of high speed photography it was found that the explosion by-products interfered with the laser beam.

[3] Visar measurements under similar conditions by Ryan (1993) have indicated comparable flyer velocities.

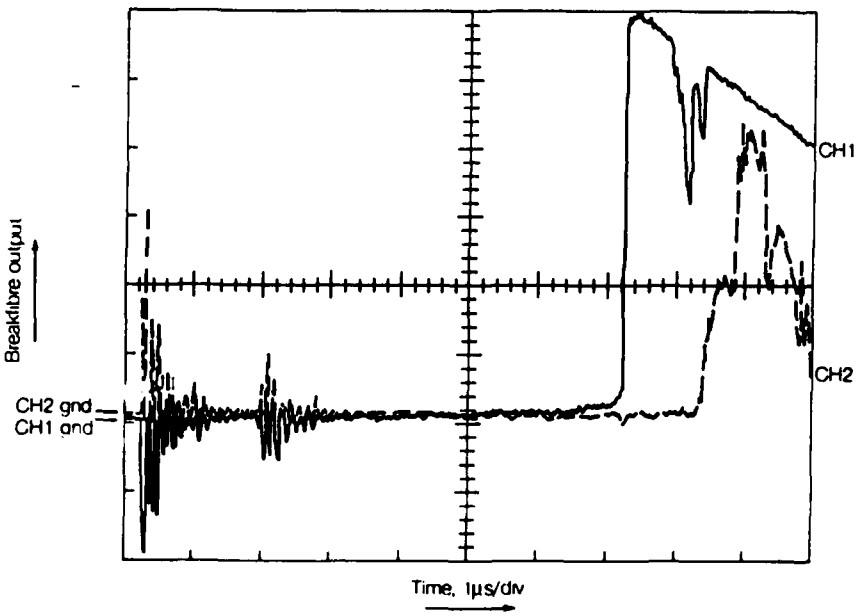

Figure 13: An example of optical breakfibre record obtained during a 5 kV shot, No. 217. The fibre separation is 3.4 mm and the position of the 1st fibre is 8 mm from the flyer origin. The time difference between fibre breaks is 1.14 µs, giving an estimated velocity of ≈ 3 km/s.

8. Conclusion

Compared with the dual breakwire method, the single breakwire technique has, under fixed conditions, produced consistent results from which an approximate flyer-velocity profile could be obtained. The arguments and experimental evidence furnished in this report lead us to believe that with an appropriate number of shots, a reasonably reliable curve of flyer velocity versus displacement can be obtained for constant initial conditions. The measurement uncertainty depends on the constancy of the launching rig performance and on the range of velocities measured, as some dependence of the intrinsic delay time in the wire break mechanism is expected. A 10% accuracy in the maximum flyer velocity determination seems achievable, though a further improvement greater than about 5% is highly unlikely.

In our analysis of the single breakwire data, we found that the consistency of the breakwire performance depended strongly on the Boomer current waveform. Therefore, it is quite conceivable that one could generate a library of flyer velocity

calibration characteristics of the Boomer rig as a function of the Boomer current waveform and eliminate the need for a direct velocity monitor. However, a considerable body of experimental data would have to be collected before such an indirect approach could be used with confidence.

Some of the chief advantages of the breakwire method are: simplicity, low cost, and useful level of accuracy. When applied to the Boomer electromagnetic launch rig, the breakwire technique performs quite well in high levels of ambient electromagnetic radio-frequency and optical noise. The disadvantages, on the other hand, consist of flyer damage caused by flyer-breakwire interaction and the need to perform a considerable number of experiments for a particular launch-rig to characterize its flyer velocity profile.

The breakwire technique is believed to be quite suitable for projectile velocity measurements above 1 km/s and well into the hypervelocity range (> 2 km/s). Future work should include the validation of the breakwire technique through other measurement methods such as the VISAR[4], and from such work, appropriate correction factors could be determined, leading to further improvements of the technique's accuracy.

9. *Acknowledgements*

The author wishes to acknowledge the advice, help and technical assistance of the following people. Drs Don Richardson and Ray Woodward, Miss Christina Olsson and Messrs Brian Jones, David Hatt, Philip Ryan, Richard Klar, Jeremy Somers, Eric Northeast, Ross Kummer and Warren Reid. The support of Mr Graeme Manzie and Dr Norbert Burman is also appreciated.

10. *References*

Barker, L.M. and Hollenbach, R.E. (1972). Laser interferometer for measuring high velocities of any reflecting surface, *Journal of Applied Physics*, Vol. 43, No. 11, pp. 4669-4675.

Chau, H.H., Dittbenner, G., Hofer, W.W., Honodel, C.A., Steinberg, D.J., Stroud, J.R. and Weingart, R.C. (1980). Electric gun: a versatile tool for high-pressure shock-wave research, *Review of Scientific Instruments*, Vol. 51, No. 12, pp. 1676-1681.

Freedman, E. and Greene, E.F. (1972). Shock waves, in *American Institute of Physics Handbook*, ed. D E. Gray, McGraw Hill, 3rd ed.

[4] The more recent VISAR results from the work by Ryan (1993) show lower flyer velocities for the Boomer II rig (refer to Podlesak *et al.* (1993) for design differences between Boomer I and Boomer II rigs) A number of factors may account for the differences including effects of bridge-foil plasma jetting. However, these would need to be investigated by more direct experimental comparisons.

Gehring, J.W. (1970). Theory of impact on thin targets and shields and correlation with experiment, in *High-Velocity Impact Phenomena*, ed. R. Kinslow. New York: Academic Press.

Harlan, J.G., Rice, J.K. and Rogers, J.W. (1981). The role of air and other gases in flyer plate initiation of explosives, *Proceedings of the 7th International Symposium on Detonation*, Annapolis, MD, pp. 930-939, 16-19 June.

Hatt, D.J. (1992). *A VISAR velocity interferometer system at MRL for slapper detonator and shockwave studies* (MRL Technical Report MRL-TR-91-42). Maribyrnong, Vic.: Materials Research Laboratory.

Herrmann, W. and Wilbeck, J. (1986). *Review of hypervelocity penetration theories* (SAND-86-1884C). Sandia National Laboratories Report.

Holian, K.S. and Holian, B.L. (1989). Hydrodynamic simulations of hypervelocity impacts, *International Journal of Impact Engineering*, Vol. 8, No. 2, pp. 115-132.

Kinslow, R. (ed.) (1970). *High-velocity impact phenomena*. New York: Academic Press.

Piekutowski, A.J. (1990). A simple dynamic model for the formation of debris clouds, *International Journal of Impact Engineering*, Vol. 10, pp. 453-471.

Podlesak, M., Richardson, D.D., Olsson, C. and Jones, B.E. (1993). *An exploding foil flying plate generator for shock wave studies - calibrations* (MRL Research Report MRL-RR-1-92). Maribyrnong, Vic.: Materials Research Laboratory.

Podlesak, M. (1990). Rogowski coil calibration on a capacitive discharge rig without the use of a current reference, *Review of Scientific Instruments*, Vol. 61, No. 2, pp. 892-896.

Rashleigh, S.C. and Marshall, R.A. (1978). Electromagnetic acceleration of microparticles to high velocities, *Journal of Applied Physics*, Vol. 49, No. 4, pp. 2540-2452.

Ryan, P.F.X. (1993). *Experimental methods in the production and measurement of shock waves in solid materials* (PhD dissertation). Canberra: Australian National University.

Ryan, P.F.X., Jones, B.J. and Richardson, D.D. (1989). *A medium scale flying plate generator design* (MRL Research Report MRL-RR-2-89). Maribyrnong, Vic.: Materials Research Laboratory.

Szajman, J., Di Marzio, F., Mazzolini, A.P. and Podlesak, M. (1989). High velocity measurements in an electromagnetically noisy environment using fibreoptic techniques, *Proceedings of the Australasian Instrumentation and Measurement Conference 1989*, Adelaide, November 14-17, pp. 14-16.

Schulz, J.C., Heimdahl, O.E.R. and Finnegan, S.A. (1987). Computer characterization of debris clouds resulting from hypervelocity impact, *International Journal of Impact Engineering*, Vol. 5, pp. 577-584.

Segletes, S. and Zukas, J.A. (1989). Simulation of high strain rate effects with microcomputers, *Proceedings of the International Conference on Mechanical Properties of Materials at High Rates of Strain*, Oxford.

Stanton, P.L. (1976). *The acceleration of flyer plates by electrically exploded foils* (Report SAND 75-0221). Sandia Laboratories.

Steinberg, D.J. (1991). *Equation of state and strength properties of selected materials* (Report No. UCID-17943). Lawrence Livermore National Laboratory, USA.

Webb, F.H., Chase, N., Ernstene, M. and Tollestrup, A. (1959). Submicrosecond wire explosion studies at Electro-optical Systems Inc., pp. 33-58, *Exploding wires*, Chace, W.G. and Moore, H.K. (eds.). New York: Plenum Press Inc.

Appendix 1

Boomer Current Waveform: Defining the Bridge-Burst Point

The definition of burst point of Boomer bridge foil is based on arguments similar to those of Webb *et al.* (1959), in their studies of exploding wires Webb *et al.* explain how a bursting wire passes through different states, namely solid, liquid and vapour, which affect its electrical resistivity in distinct ways. In our own experiments we have observed that the resistance of the foil rises practically exponentially through the solid, liquid and vapour state. In the vapour state the foil resistance is at its highest.

It is at this point of total vaporization that the foil gas experiences the greatest confinement and pressure, which in turn forms and accelerates the flyer plate towards the target. The liquid to vapour transition of state is closely correlated with the sudden decrease in foil current, since the non-ionized or weakly ionized aluminium vapour is quite resistive compared with its solid or liquid phase. Webb *et al.* note that for aluminium, the temperature of vaporization is considerably lower than that of its ionization.

Hence, as the foil approaches the point of total vaporization it experiences the greatest rise in its total electrical resistance. This occurs approximately at the point of maximum rate of decrease in Boomer current, as shown below.

Electrically, the Boomer apparatus can be represented in terms of three lumped parameters, namely capacitance, C, inductance, L, and resistance $(R + r(t))$, where R is the system resistance and $r(t)$ is the time dependent bridge-foil resistance. When the Boomer capacitor is charged to an initial voltage V_0 and then discharged through the bridge-foil, the current $i(t)$ in the circuit obeys the following second order differential equation. Neglecting switch resistance, we have

$$-L\,i'(t)-(R+r(t))\,i(t)-(1/C)\int_{t=0}^{t} i(t)dt+V_0=0, \qquad \text{(A1)}$$

where the prime symbol denotes differentiation with respect to time, d/dt.

The bursting foil acts as a fast opening switch and it will give rise to a large reactive voltage component due to inductively stored energy in the circuit. Thus at large rates of current change and with the foil resistance dominating the overall circuit resistance, Eq. (A1) reduces to

$$L\,i'(t) \;=\; -r(t)\,i(t). \qquad \text{(A2)}$$

During this opening phase, the voltage across the bridge, $v(t) = -r(t)\ i(t)$, is chiefly provided by the inductive reactance of the circuit ($L\,i'(t)$), and is therefore closely related to the rapid change in bridge resistance due to foil vaporization. Since, according to experimental evidence, the rise in resistance is nearly exponential, then the maximum rate of current decrease occurs at the peak voltage across the bridge, and coincides with the final phase of foil vaporization. We define this point in time according to

$$L\, i''(t_b) = -v'(t_b) \quad = \quad 0 \tag{A3}$$

where t_b is the time of bridge-burst, at which $i'(t)$ has its first minimum.

Appendix 2

Shock Hugoniot Parameters for Copper and Polycarbonate

Table 3: Shock Hugoniot parameters from (Steinberg, 1991) according to equation $U_s = c_o + s\,u_p$, *where* U_s *is the shock velocity,* c_o *the speed of sound in unshocked material,* u_p *the particle velocity and s a material dependent proportionality constant*

Material	Unshocked density (kg m^{-3})	c_o (km/s)	s
Copper	8930	3.94	1.49
Polycarbonate	1196	1.93	3.49

SECURITY CLASSIFICATION OF THIS PAGE UNCLASSIFIED

REPORT NO.	AR NO	REPORT SECURITY CLASSIFICATION
MRL-TR-92-39	AR-008-223	Unclassified

TITLE

Breakwire technique for hypervelocity measurement

AUTHOR(S)
Michael Podlesak

CORPORATE AUTHOR
DSTO Materials Research Laboratory
PO Box 50
Ascot Vale Victoria 3032

REPORT DATE	TASK NO.	SPONSOR
September, 1993	DST	DSTO

FILE NO.	REFERENCES	PAGES
G6/4/8-4068	22	44

CLASSIFICATION/LIMITATION REVIEW DATE

CLASSIFICATION/RELEASE AUTHORITY
Chief, Explosives Ordnance Division

SECONDARY DISTRIBUTION

Approved for public release

ANNOUNCEMENT

Announcement of this report is unlimited

KEYWORDS

Hypervelocity Measurement Flying Plate Breakwire

ABSTRACT

An electrical breakwire technique for measuring the speed of hypervelocity projectiles is described and assessed, using Boomer, a large scale exploding foil flying plate generator. Two techniques were tested, a dual breakwire method and a single breakwire method. The dual breakwire method is the simpler of the two, but it was found to be less reliable than the single breakwire approach. With the single breakwire method, a reasonable approximation to the projectile's velocity-time-history can be obtained by conducting a series of experiments where a range of times of arrival of the flyer is measured as a function of the breakwire position only. However, accuracy of this technique depends on shot-to-shot consistency and the velocity versus time resolution is limited by the number of different positions of the projectile's trajectory at which the firings can be performed. Compared with other velocity measurement techniques, the breakwire method was found reasonably consistent and effective, in terms of simplicity, turnaround time, low cost and ability to operate within an environment containing high levels of electromagnetic noise in the radio-frequency and optical spectrum. Analysis of the breakwire data from Boomer experiments has indicated a possibility of improvement in the accuracy of the single breakwire technique through correlation of the time-of-break with variations in the Boomer-current waveform.

SECURITY CLASSIFICATION OF THIS PAGE
UNCLASSIFIED

Breakwire Technique for Hypervelocity Measurement

Michael Podlesak

(MRL-TR-92-39)

DISTRIBUTION LIST

Director, MRL
Chief, Explosive Ordnance Division
Dr D.D. Richardson
Dr Michael Podlesak
MRL Information Service

Chief Defence Scientist (for CDS, FASSP, ASSCM) (1 copy only)

Director (for Library), Aeronautical Research Laboratory

Head, Information Centre, Defence Intelligence Organisation
OIC Technical Reports Centre, Defence Central Library
Officer in Charge, Document Exchange Centre (8 copies)
Army Scientific Adviser, Russell Offices
Air Force Scientific Adviser, Russell Offices
Navy Scientific Adviser, Russell Offices - data sheet only
Scientific Adviser, Defence Central
Director-General Force Development (Land)
Senior Librarian, Main Library DSTOS
Librarian, MRL Sydney
Librarian, H Block
UK/USA/CAN ABCA Armies Standardisation Rep. c/- DGAT
Librarian, Australian Defence Force Academy
Counsellor, Defence Science, Embassy of Australia - data sheet only
Counsellor, Defence Science, Australian High Commission - data sheet only
Scientific Adviser to DSTC, C/- Defence Adviser - data sheet only
Scientific Adviser to MRDC, C/- Defence Attache - data sheet only
Head of Staff, British Defence Research and Supply Staff (Australia)
NASA Senior Scientific Representative in Australia
INSPEC: Acquisitions Section Institution of Electrical Engineers
Head Librarian, Australian Nuclear Science and Technology Organisation
Senior Librarian, Hargrave Library, Monash University
Library - Exchange Desk, National Institute of Standards and Technology, US
Exchange Section, British Library Document Supply Centre
Periodicals Recording Section, Science Reference and Information Service, UK
Library, Chemical Abstracts Reference Service
Engineering Societies Library, US
Documents Librarian, The Center for Research Libraries, US

Gil Smith, EOD
David Hatt, EOD
Mick Chick, EOD
Phil Ryan, SSMD
John Howe, SSMD
Christine Olsson, ARL
Dr Jakob Sczajman, Victoria University of Technology, Dept. of Applied Physics